



1

Local active information storage as a tool to understand distributed neural information processing

Michael Wibral^{1,*}, Joseph T. Lizier², Sebastian Vögler³, Viola Priesemann⁴,
and Ralf Galuske³

¹MEG Unit, Brain Imaging Center, Goethe University, Frankfurt am Main, Germany

²CSIRO Computational Informatics, Marsfield, NSW, Australia

³Fakultät für Biologie, Technische Universität, Darmstadt, Germany

⁴Max Planck Institute for Dynamics and Self-Organization, Göttingen, Germany

Correspondence*:

Michael Wibral

MEG Unit, Brain Imaging Center, Goethe University, Heinrich-Hoffmann Strasse
10, Frankfurt am Main, D-602528, Germany, wibral@em.uni-frankfurt.de

Information-based methods for neuroimaging: analyzing structure, function
and dynamics

2 ABSTRACT

3 Every act of information processing can in principle be decomposed into the component
4 operations of information storage, transfer, and modification. Yet, while this is easily done for
5 today's digital computers, the application of these concepts to neural information processing
6 was hampered by the lack of proper mathematical definitions of these operations on information.
7 Recently, definitions were given for the dynamics of these information processing operations on
8 a local scale in space and time in a distributed system, and the specific concept of local active
9 information storage was successfully applied to the analysis and optimization of artificial neural
10 systems. However, no attempt to measure the space-time dynamics of local active information
11 storage in neural data has been made to date. Here we measure local active information storage
12 on a local scale in time and space in voltage sensitive dye imaging data from area 18 of the cat.
13 We show that storage reflects neural properties such as stimulus preferences and surprise upon
14 unexpected stimulus change, and in area 18 reflects the abstract concept of an ongoing stimulus

15 despite the locally random nature of this stimulus. We suggest that LAIS will be a useful quantity
16 to test theories of cortical function, such as predictive coding.

17 **Keywords:** Visual System, Neural Dynamics, Predictive Coding, Local Information Dynamics, Voltage Sensitive Dye Imaging,
18 Distributed Computation, Complex Systems, Information Storage

1 INTRODUCTION

19 It is commonplace to state that brains exist to ‘process information’. Curiously enough, however, it is
20 much more difficult to exactly quantify this putative processing of information. In contrast, we have
21 no difficulties to quantify information processing in a digital computer, e.g. in terms of the information
22 stored on its hard disk, or the amount of information transferred per second from its hard disk to its random
23 access memory, and then on to the CPU. Why then is it so difficult to perform a similar quantification for
24 biological, and especially neural information processing?

25 One answer to this question is the conceptual difference between a digital computer and a neural system:
26 In a digital computer all components are laid out such that they only perform specific operations on
27 information: a hard disk should store information, and not modify it, while the CPU should quickly
28 modify the incoming information and then immediately forget about it, and system buses exist solely
29 to transfer information. In contrast, in neural systems it is safe to assume that each element of the
30 system (each neuron) *simultaneously* stores, transfers and modifies information in variable amounts,
31 and the component processes are hard to separate quantitatively. Thus, while in digital computers the
32 distinction between information storage, transfer and modification comes practically for free, in neural
33 systems separating the components of distributed information processing requires thorough mathematical
34 definitions of information storage, transfer and modification. Such definitions, let alone a conceptual
35 understanding of what the terms meant in distributed information processing, were unavailable until very
36 recently (Langton, 1990; Mitchell, 1998; Lizier, 2013).

37 These necessary mathematical definitions were recently derived building on Turing’s old idea that every
38 act of information processing can be decomposed into the component processes of information storage,
39 transfer and modification (Turing, 1936) – very much in line with our everyday view of the subject.
40 Later, Langton and others expanded Turing’s concepts to describe the emergence of the capacity to
41 perform arbitrary information processing algorithms, or ‘universal computation’, in complex systems,
42 such as cellular automata (Langton, 1990; Mitchell et al., 1993), or neural systems. The definitions of
43 information transfer and storage were then given by Schreiber (2000), Crutchfield and Feldman (2003)
44 and Lizier et al. (2012b). However, the definition of information modification is still a matter of debate
45 (Lizier et al., 2013).

46 Of these three component processes above – information transfer, storage, and modification –
47 information storage in particular has been used with great success to analyze cerebro-vascular dynamics
48 (Faes et al., 2013), information processing in swarms (Wang et al., 2012), and most importantly, to
49 evolve (Prokopenko et al., 2006), and optimize (Dasgupta et al., 2013) artificial information processing
50 systems. This suggests that the analysis of information storage could also be very useful for the analysis
51 of neural systems.

52 Yet, while neuroscientists have given much attention to considering how information is stored
53 structurally in the brain, e.g. via synaptic plasticity, the same attention has not been given to information
54 storage in neural dynamics, and its quantification. As an exception Zipser et al. (1993) clearly contrasted
55 two different ways of storing information: *passive storage*, where information is stored “in modified
56 values of physiological parameters such as synaptic strength”, and *active storage* where “information
57 is preserved by maintaining neural activity throughout the time it must be remembered”. In the same
58 paper, the authors go on to point out that there is evidence for the use of both storage strategies in higher
59 animals, and link the relatively short time scale for active storage (at maximum in the tens of seconds)
60 with short-term or working memory and, therefore, refer to it as “active information storage”.

61 Despite the importance of information storage for neural information processing, information theoretic
62 measures of active information storage have not yet been used to quantify information processing in
63 neural systems, and in particular not to measure spatiotemporal patterns of information storage dynamics.
64 Therefore, it is the aim of this article to introduce measures of information storage as analysis tools for
65 the investigation of neural systems, and to demonstrate how cortical information storage in visual cortex
66 unfolds in space and time. We will also demonstrate how neural activity may be misinformative about its
67 own future and thereby generates ‘surprise’.

68 To this end, we first give a rigorous mathematical definition of information storage in dynamic activity
69 in the form of local active information storage (LAIS). We then show how to apply this measure to voltage
70 sensitive dye imaging data from cat visual cortex. In these data, we found sustained increases in dynamic
71 information storage during visual stimulation, organized in clear spatiotemporal patterns of storage across
72 the cortex, including stimulus-specific spatial patterns, and negative storage, or surprise, upon a change of
73 the stimulus. Finally, we discuss the implications of the LAIS measure for neurophysiological theories of
74 predictive coding (see Bastos et al. (2012), and references therein), that have been suggested to explain
75 general operating principles of the cortex and other hierarchical neural systems.

2 MATERIAL & METHODS

76 The use of the stored information for information processing inevitably requires its re-expression in neural
 77 activity and its interaction with ongoing neural activity and incoming information. Hence, information
 78 storage *actively in use for information processing* will inevitably be reflected in the dynamics of neural
 79 activity, and is therefore accessible in recordings of neural activity alone. To quantify this stored
 80 information that is present in neural time series we will now introduce a measure of information storage
 81 called *local active information storage* (Lizier et al., 2012b). In brief, this measure quantifies the amount
 82 of information in a sample from a neural time series that is predictable from its past – and thereby has
 83 been stored in this past. This is done by simply computing the local mutual information between the past
 84 of a neural signal and its next sample at each point in time, and for each channel of a recording. As the
 85 following material is necessarily formal, the reader may consider skipping ahead to section 2.2.3 at first
 86 reading to gain an intuitive understanding of mechanisms that serve active information storage.

2.1 NOTATION AND INFORMATION THEORETIC PRELIMINARIES

87 To avoid confusion, we first have to state how we formalize observations from neural systems
 88 mathematically. We define that a neural (sub-)system of interest (e.g. a neuron, or brain area) \mathcal{X} produces
 89 an observed time series $\{x_1, \dots, x_t, \dots, x_N\}$, sampled at time intervals δ . For simplicity we choose our
 90 temporal units such that $\delta = 1$, and hence index our measurements by $t \in \{1 \dots N\} \subseteq \mathbb{N}$, i.e. we index
 91 in terms of samples. The full time series is understood as a realization of a *random process* X . This
 92 random processes is nothing but a collection of random variables X_t , sorted by an integer index (t in our
 93 case). Each random variable X_t , at a specific time t , is described by the set of all its J possible outcomes
 94 $\mathcal{A}_{X_t} = \{a_1, \dots, a_j, \dots, a_J\}$, and their associated probabilities $p_t(x_t = a_j)$. The probabilities of a specific
 95 outcome $p_t(x_t = a)$ may change with t , i.e. when going from one random variable to the next. In this
 96 case, we will indicate the specific random variable X_t the probability distribution belongs to – hence the
 97 subscript in $p_t(\cdot)$. For practical estimation of $p_t(\cdot)$ then, multiple time-series realizations or trials would
 98 be required. For stationary processes, where $p_t(x_t = a)$ does not change with t , we simply write $p(x_t)$,
 99 and practical estimation may be done from a single time-series realization. In sum, in this notation the
 100 individual random variables X_t produce realizations x_t , and the time-point index of a random variable X_t
 101 is necessary when the random process is nonstationary. When using more than one system, the notation is
 102 generalized to multiple systems $\mathcal{X}, \mathcal{Y}, \mathcal{Z}, \dots$.

103 As we will see below, active information storage is nothing but a specific mutual information between
 104 collections of random variables in the process in question. We therefore start by giving the definition of
 105 *mutual information* (MI) $I(X; Y)$ as the amount of information held in common by two random variables
 106 U, V on average (Cover and Thomas, 1991):

$$I(U; V) = \sum_{u \in \mathcal{A}_U, v \in \mathcal{A}_V} p(u, v) \log \frac{p(u, v)}{p(u)p(v)}, \quad (1)$$

$$= \sum_{u \in \mathcal{A}_U, v \in \mathcal{A}_V} p(u, v) \log \frac{p(v | u)}{p(v)}, \quad (2)$$

107 where the log can be taken to an arbitrary base, and choosing base 2 yields the mutual information in
 108 bits. Note that the mutual information $I(U; V)$ is symmetric in U and V . As shown more explicitly in
 109 equation 2, the MI $I(U; V)$ measures the amount of information provided (or the amount that uncertainty
 110 is reduced) by an observation of a specific outcome u of the variable U about the occurrence of another
 111 specific outcome v of V - on average over all possible values of u and v . As originally pointed out by
 112 **Fano** (1961), the summands $\log \frac{p(v|u)}{p(v)}$ have a proper interpretation even without the weighted averaging
 113 – as the information that observation of a specific u provides about the occurrence of a specific v . The
 114 *pointwise* or *local mutual information* is therefore defined as:

$$i(u; v) = \log \frac{p(v | u)}{p(v)}. \quad (3)$$

115 It is important to note the distinction of the local mutual information measure $i(x; y)$ considered here
 116 from partial localization expressions, i.e. the partial mutual information or specific information $I(u; V)$
 117 which are better known in neuroscience (**DeWeese and Meister**, 1999; **Butts**, 2003; **Butts and Goldman**,
 118 2006). Partial MI expressions consider information contained in specific values u of one variable U about
 119 the other (unknown) variable V . Crucially, there are two valid approaches to measuring partial mutual
 120 information, one which preserves the additivity of information and one which retains non-negativity
 121 (**DeWeese and Meister**, 1999). In contrast, the fully local mutual information $i(x; y)$ that is used here
 122 is uniquely defined as shown by **Fano** (1961).

2.2 LOCAL ACTIVE INFORMATION STORAGE

123 Using the definition in equation 3, we can immediately quantify how much of the information in in the
 124 outcome x_t of the random variable X_t at time t was predictable from the observed past *state* \mathbf{x}_{t-1}^{k-} of the
 125 process at time $t - 1$:

$$a(x_t) = i(\mathbf{x}_{t-1}^{k-}; x_t) \quad (4)$$

$$= \log \frac{p_t(x_t | \mathbf{x}_{t-1}^{k-})}{p_t(x_t)}. \quad (5)$$

126 This quantity was introduced by **Lizier et al.** (2012b) and called *local active information storage*
 127 (LAIS). Here, \mathbf{x}_{t-1}^{k-} is an outcome of the collection of previous random variables $\mathbf{X}_{t-1}^{k-} =$
 128 $\{X_{t-1}, X_{t-t_1}, \dots, X_{t-t_{k_{max}}}\}$, called a *state* (see below). The corresponding expectation value over all
 129 possible observations of x_t and \mathbf{x}_{t-1}^{k-} , $A(X_t) = I(\mathbf{X}_{t-1}^{k-}; X_t)$, is known simply as the *active information*
 130 *storage*. The naming of this measure aligns well with the concept of active storage in neuroscience
 131 by **Zipser et al.** (1993), but is more general than capturing only sustained firing patterns. In the
 132 following subsections, we comment on practical issues involved in estimating the LAIS, and discuss
 133 its interpretation.

134 *2.2.1 Interpretation and construction of the past state* As indicated above, the joint variable
 135 \mathbf{x}_{t-1}^{k-} in (equation 4) is an outcome of the collection of previous random variables: $\mathbf{X}_{t-1}^{k-} =$
 136 $\{X_{t-1}, X_{t-t_1}, \dots, X_{t-t_{k_{max}}}\}$. This collection should be constructed such, that it captures the *state* of
 137 the underlying dynamical system \mathcal{X} , and can be viewed as a state-space reconstruction of this system. In
 138 this sense, \mathbf{X}_{t-1}^{k-} must be chosen such that X_t is conditionally independent of all X_{t-t_l} with $t_l > t_{k_{max}}$,
 139 i.e. of all variables that are observed earlier in the process \mathbb{X} than the variables in the state at $t - 1$.
 140 The choice must be made carefully, since using too few variables X_{t-t_l} from the history can result
 141 in an underestimate of $a(x_t)$, while using too many (given the amount of data used to estimate the
 142 probability density functions (PDFs) in (equation 4)) will artificially inflate it. Typically, the state can be
 143 captured via Takens delay embedding (**Takens**, 1981), using d variables X_{t-t_l} with the t_l delays equally
 144 spaced by some $\tau \geq 1$, with d and τ selected using the Ragwitz criteria (**Ragwitz and Kantz**, 2002)
 145 – as recommended by **Vicente et al.** (2011) for the related transfer entropy measure (**Schreiber**, 2000).
 146 Alternatively, non-uniform embeddings may be used (e.g. see **Faes et al.** (2012)).

If the process has infinite memory, and k_{max} does not exist, then the local active information storage is defined as the limit $\lim_{k \rightarrow \infty}$ of equation 4:

$$a(x_t) = \lim_{k \rightarrow \infty} i(\mathbf{x}_{t-1}^{k-}; x_t) \quad (6)$$

$$= \lim_{k \rightarrow \infty} \log \frac{p_t(x_t | \mathbf{x}_{t-1}^{k-})}{p_t(x_t)}. \quad (7)$$

147 2.2.2 *Relation to other measures and dynamic state updates* The average active information storage
 148 (AIS), is related to two measures introduced previously. On the one hand, a similar measure called
 149 'regularity' had been introduced by **Porta et al.** (2000). On the other hand, AIS is closely related to
 150 the excess entropy (**Crutchfield and Feldman**, 2003), as observed in (**Lizier et al.**, 2012b). The excess
 151 entropy $E(X_t) = I(\mathbf{X}_{t-1}^{k-}; \mathbf{X}_t^{k+})$, with $\mathbf{X}_t^{k+} = \{X_t, X_{t+t_1}, \dots, X_{t+t_{kmax}}\}$ being a similar collection of
 152 future random variables from the process, measures the amount of information (on average) in the future
 153 outcomes \mathbf{x}_t^{k+} of the process this is predictable from the observed past state \mathbf{x}_{t-1}^{k-} at time $t - 1$. As such,
 154 the excess entropy captures all of the information in the future of the process that is predictable from
 155 its past. In measuring the subset of that information in only the next outcome of the process, the AIS is
 156 focused on the dynamic state updates of the process.

157 From the point of view of dynamic state updates, the AIS is *complementary* to a well-known measure
 158 of uncertainty of the next outcome of the process which cannot be resolved by its past state. Following
 159 **Crutchfield and Feldman** (2003) we refer to this quantity as the "entropy rate", the conditional entropy
 160 of the next outcome given the past state: $H_\mu(X_t) = H(X_t | \mathbf{X}_{t-1}^{k-}) = \langle -\log_2 p_t(x_t | \mathbf{x}_{t-1}^{k-}) \rangle$. The
 161 complementarity of the entropy rate and AIS was shown by **Lizier et al.** (2012b): $H(X_t) = A(X_t) +$
 162 $H_\mu(X_t)$, where $H(X_t)$ is the Shannon entropy of the next measurement X_t . $H_\mu(X_t)$ is approximated
 163 by measures known as the Approximate Entropy (**Pincus**, 1991), Sample Entropy (**Richman and**
 164 **Moorman**, 2000), and Corrected Conditional Entropy (**Porta et al.**, 1998), which have been well studied
 165 in neuroscience (see e.g. the work by **Vakorin et al.** (2011); **Gómez and Hornero** (2010), and references
 166 therein). Many such studies refer to $H_\mu(X_t)$ as a measure of complexity, however modern complex
 167 systems perspectives focus on complexity as being captured in how much structure can be resolved rather
 168 than how much cannot (**Crutchfield and Feldman**, 2003).

169 Furthermore, given that the most appropriate measure of complexity of a process is a matter of open
 170 debate (**Prokopenko et al.**, 2009), we take the perspective that complexity of a system is best approached
 171 as arising out of the interaction of the component operations of information processing: information
 172 storage, transfer and modification (**Lizier**, 2013), and focus on measuring these quantities since they are
 173 rigorously defined and well-understood. Crucially, in comparison to the excess entropy discussed above,
 174 the focus of AIS in measuring the information storage in use in dynamic state updates of the process make
 175 it directly comparable with measures of information storage and modification. Of particular importance
 176 here is the relationship of AIS to the transfer entropy (**Schreiber**, 2000), where the two measures together
 177 reveal the sources of information (either being the past of that process itself – storage, or of other processes
 178 – transfer) which contribute to prediction of the process' next outcome.

179 The formulation of the transfer entropy specifically eliminates information storage in the past of the
 180 target process from being mistakenly considered as having been transferred (**Lizier**, 2013; **Lizier and**

181 **Prokopenko**, 2010; **Wibral et al.**, 2013). An interesting example is where a periodic target process is
182 in fact causally driven by another periodic process – after any initial entrainment period, our information
183 processing view concludes that we have information storage here in the target but no transfer from the
184 driver (**Lizier and Prokopenko**, 2010). While causally there is a different conclusion, our observational
185 information processing perspective is simply focussed on decomposing apparent information sources of
186 the process, regardless of underlying causality (which in practise cannot often be determined anyway).
187 In this view, a causal interaction can computationally subserve both information storage or transfer (as
188 discussed further in the next section). Information transfer is necessarily linked to a causal interaction, but
189 the reverse is not true. It has previously been demonstrated that the information processing perspective is
190 more relevant to emergent information processing structure in complex systems, e.g. coherent information
191 cascades, in contrast to causal interactions being more relevant to the micro-scale physical structure of a
192 system, e.g. axons in a neural system (**Lizier and Prokopenko**, 2010).

193 *2.2.3 Mechanisms producing active information storage* In contrast to passive storage in terms of
194 modifications to system structure (e.g. synaptic gain changes), the mechanisms underlying active
195 information storage are not immediately obvious. The mechanisms that subserve this task have been
196 formally established however, and can be grouped as follows:

- 197 1. *Physical mechanisms in the system.* This could incorporate some internal memory mechanism in the
198 individual physical element giving rise to the process X (e.g. some decay function, or the stereotypical
199 processes during the refractory period after a neural spike). More generally, it may involve network
200 structures which offload or distribute the memory function onto edges or other nodes. In particular,
201 **Zipser et al.** (1993) reported that networks with fixed, *recurrent connections* were sufficient to
202 account for such active storage patterns, which is in line with earlier proposals. Furthermore, **Lizier**
203 **et al.** (2012a) quantified the AIS contribution from self-loops, feedback and feedforward loops (as
204 the only network structures contributing to active information storage).
- 205 2. *Input-driven storage.* This describes situations where the apparent memory in the process is caused
206 by information storage structure which lies in another element which is driving that process, e.g. a
207 periodically spiking neuron that may cause a downstream neuron to spike with the same period (**Obst**
208 **et al.**, 2013). As described in Section 2.2.2 above, an observer of the process attributes these dynamics
209 to information storage, regardless of the (unobserved) underlying causal mechanism.

210 Of these mechanisms of active information storage the case of circular causal interactions in a loop motif,
211 and the causal, but repetitive influence from another part of the system may seem counterintuitive at first,
212 as we might think that in these cases there should be information transfer rather than active information

213 storage. To see why these interactions serve storage rather than transfer, it may help to consider that *all*
214 components of information processing, i.e. transfer, active storage and modification, ultimately have to
215 rely on causal interactions in physical systems. Hence, the presence of a causal interaction cannot be linked
216 in a one-to-one fashion to information transfer, as otherwise there would be no possibility for physical
217 causes of active information storage and of information modification left, and no consistent decomposition
218 of information processing would be possible. Therefore, the notion of storage that is measurable in a part
219 of the system but that can be related to external influences onto that part is to be preferred for the sake of
220 mathematical consistency and ultimately, usefulness. We acknowledge that information transfer has often
221 been used as a proxy for a causal influence, dating back to suggestions by **Wiener** (1956) and **Granger**
222 (1969). However, now that causal interventional measures and measures of information transfer can be
223 clearly distinguished (**Lizier and Prokopenko**, 2010; **Ay and Polani**, 2008) it seems no longer warranted
224 to map causal interactions to information transfer in a one-to-one manner.

225 *2.2.4 Interpretation of LAIS values* Measurements of the LAIS tells us the amount to which observing
226 the past state \mathbf{x}_{t-1}^{k-} reduced our uncertainty about the specific next outcome x_t that was observed. We can
227 interpret this in terms of *encoding* the outcome x_t in bits: encoding x_t using an optimal encoding scheme
228 for the distribution $p_t(x_t)$ takes $-\log_2 p_t(x_t)$ bits, whereas encoding x_t if we know \mathbf{x}_{t-1}^{k-} using an optimal
229 encoding scheme for the distribution $p_t(x_t | \mathbf{x}_{t-1}^{k-})$ takes $-\log_2 p_t(x_t | \mathbf{x}_{t-1}^{k-})$ bits, and the LAIS is the
230 number of bits saved via the latter approach.

231 At first glance we may assume that the LAIS is a positive quantity. Indeed, as a mutual information,
232 the *average* AIS will always be non-negative. However, the LAIS can be negative as well as positive.
233 It is positive where $p_t(x_t | \mathbf{x}_{t-1}^{k-}) > p_t(x_t)$, i.e. where the observed past state \mathbf{x}_{t-1}^{k-} made the following
234 observation x_t more likely to occur than we would have guessed without the knowledge of the past state.
235 In this case, we state that \mathbf{x}_{t-1}^{k-} was *informative*. In contrast, the LAIS is negative where $p_t(x_t | \mathbf{x}_{t-1}^{k-}) <$
236 $p_t(x_t)$; i.e. where the observed past state \mathbf{x}_{t-1}^{k-} made the following observation x_t less likely to occur than
237 we would have guessed without the knowledge of the past state (but it occurred nevertheless, making the
238 cue given by \mathbf{x}_{t-1}^{k-} misleading). In this case, we state that \mathbf{x}_{t-1}^{k-} was *misinformative* about x_t . To better
239 understand negative LAIS also see the further discussion in (**Lizier et al.**, 2012a), including examples in
240 cellular automata where the past state of a variable was misinformative about the next observation due to
241 the strong influence of an unobserved other source variable at that time point.

242 *2.2.5 Choice of the overall time window for constructing probability densities from data* As already
243 pointed out above, active information storage is tightly related to predictability of a given brain area's
244 output as seen by the receiving brain area. This predictability hinges on the ability of the receiver to
245 see the past states in the output of a brain area (see previous section) and to interpret the past states in

246 the received time series in order to make a prediction about the next value. In other words, the receiver
 247 needs to guess $p_t(x_t, \mathbf{x}_{t-1}^k)$ correctly in order to exploit the active information storage. If the guess of the
 248 receiving neuron (n) or brain area, i.e. $\tilde{p}_n(x_t, \mathbf{x}_{t-1}^k)$, is incorrect, then only a fraction of the information
 249 storage can be used for successfully predicting future events. The losses could be quantified as the extra
 250 coding cost for the receiving area, when assuming $\tilde{p}_n(\cdot)$ instead of $p_t(\cdot)$. This loss would simply be
 251 the Kullback-Leibler divergence $D_{KL}(p_t || \tilde{p}_n)$. This scenario sees the receiving brain area mostly as an
 252 optimal encoder or compressor. In contrast, the cost occurring in the framework of predictive coding
 253 theories would arise because the receiving brain area could not predict the incoming signal well, and
 254 thereby inhibit it via feedback to the sending brain area (**Rao and Ballard**, 1999). In this scenario, the
 255 cost of imperfect predictions resulting from using \tilde{p}_n instead of p_t , would be reduced inhibition and a
 256 more frequent signaling of prediction errors by the sending system, leading to a metabolic cost.

257 To see the storage that the receiving brain area can exploit, the time interval used for the practical
 258 estimation of the probability density functions (PDFs) from neural recordings should best match the
 259 expected sampling strategy of the receiving brain area. For example, if we think that probabilities are
 260 evaluated over long time frames, then it might make sense to pool all available data in the experiment,
 261 as even a mis-estimation of the true probability densities $p_t(\cdot)$ (due to potential nonstationarities) then
 262 will better reflect the internal estimate $\tilde{p}_n(x_t, \mathbf{x}_{t-1}^k)$, and thus the *internally* predictable information.
 263 However, if we think that probabilities are only estimated instantaneously by pooling over all available
 264 inputs to a brain area at any time point, then we should construct the necessary PDFs only from all
 265 simultaneously acquired data from all measurement channels, but not pool over time. The latter view
 266 could also be described as assuming that the brain area receiving the signals in question computes the PDF
 267 instantaneously by pooling over all its inputs, without keeping any longer term memory of the observed
 268 probabilities. This construction of a PDF would be linked closely to an instantaneous physical ensemble
 269 approach, considering that all incoming channels are physically equivalent, but are only assessed at a
 270 single instant in time. In contrast, if we assume that learning of the relevant PDFs takes place on a
 271 lifelong timescale, then PDFs should be acquired from very long recordings of a freely behaving subject
 272 or animal in a natural environment, and the outcomes of a specific experiment should be interpreted using
 273 this ‘lifelong’ PDF. Here we lean towards this latter approach and pool all available data to estimate the
 274 internally available \tilde{p}_n .

275 Note that while we indeed pool over all the available data to obtain the distribution \tilde{p}_n , the interpretation
 276 of the data in terms of the active information storage is *local per agent and time step*. This is exactly the
 277 meaning of ‘local’ in local active information storage as introduced in (**Lizier et al.**, 2012b) (this is also
 278 akin to the relation of the local mutual information introduced by **Fano** (1961) and the corresponding
 279 global PDF). The local active information storage values are thus obtained by interpreting realizations for
 280 a single agent and a single time step in the light of a probability distribution that is obtained over a more

281 global view of the system in space and time. This is also indicated by the use of \tilde{p}_n instead of p_t . Also see
282 the discussion for potential other choices of obtaining p .

2.3 ACQUISITION OF NEURAL DATA

283 *2.3.1 Animal preparation* Data were obtained from an anesthetized cat. The animal had been
284 anesthetized and artificially ventilated with a mixture of O₂ and N₂O (30/70 %) supplemented with
285 Halothane (0.7 %). All procedures were along the guidelines of the Society for Neuroscience, in
286 accordance with the German law for the protection of laboratory animals, permitted by the local authorities
287 and overseen by a designated veterinarian.

288 *2.3.2 Voltage sensitive dye imaging* For optical imaging the visual cortex (area 18) was exposed and an
289 imaging chamber was implanted over the craniotomy. The chamber was filled with silicone oil and sealed
290 with a glass plate. A voltage sensitive dye (RH1691, Optical Imaging Ltd, Rehovot, Israel) was applied to
291 the cortex for about 2 hours and subsequently the excess of the dye was washed out. For imaging we used
292 a CMOS camera system (Imager 3001, Optical Imaging Ltd, Rehovot, Israel, Camera: Photon Focus MV1
293 D1312, chip size 1312x1082 pixel) fitted with a lens system consisting of two 50mm Nikon objectives
294 providing a field of view of 8.7x10.5mm and an epifluorescence illumination system (excitation: 630+/-
295 10nm, emission high pass 665nm). In order to optimize the signal-to-noise ratio raw camera signals were
296 spatially binned to 32x32 camera pixels allowing for a spatial resolution of 30x32 μm^2 per data pixel.
297 Camera frames were collected at a rate 150Hz, resulting in a temporal resolution of 6.7ms.

298 *2.3.3 Visual stimulation* Stimuli were presented triggered to the heartbeat of the animal for 2s and
299 camera frames were collected during the entire stimulation period. We will denote such a single
300 stimulation period and the corresponding data acquisition as a trial here. Each trial consisted of 1s
301 stimulation with an isoluminant grey screen followed by stimulation with fields of randomly positioned
302 dots (dot size: 0.23° visual angle; 384 dots distributed over an area of 30° (vertical) by 40° (horizontal)
303 visual angle) moving coherently in one of 8 different directions at 16 degree/s. Stimuli were presented
304 in blocks of 16 trials, consisting of 8 trials using the stimuli described before and an additional 8 trials
305 which consisted only of the presentation of the isoluminant grey screen for 2s ('blank trials'). Each motion
306 direction condition was presented 8 times in total (8 trials), resulting in the presentation on 64 stimulus
307 trials and 64 blank trials in total. Of the presented set of 8 stimulus types, 7 were used for the final analysis,
308 as the computational process for one condition did not finish on time before local compute clusters were
309 taken down for service.

310 2.3.4 *VSD data post-processing* After spatial binning of 32 x 32 camera pixels into one data pixel,
311 VSD data were averaged over all presentations of blank trials and this average was subtracted from the
312 raw data to remove the effects of dye-bleaching and heartbeat. Finally, the data were denoised using a
313 median filter of 3x3 data pixels.

2.4 MEASUREMENT OF LAIS ON VSD NEURAL DATA

314 Estimation of LAIS was performed using the open source *Java information dynamics toolkit* (JIDT)
315 (Lizier, 2012), with a history parameter k_{max} of ten time points, spaced 2 samples, or $(2/150Hz) =$
316 $13.\bar{3}$ ms, apart. The total history length thus covered 133 ms, or roughly one cycle of a neural
317 theta oscillation, which seems to be a reasonable time horizon for a downstream neural population that
318 ultimately must assess these states. To enable LAIS estimation from a sufficient amount of samples, we
319 considered the data pixels as homogeneous variables executing comparable state transitions, such that
320 the pixels form a physical ensemble in terms of information storage dynamics. Pooling data over pixels
321 thus enables an ensemble estimate of the PDFs in question. This approach seems justified as all pixels
322 reported activity from a single brain area (area 18 of cat visual cortex, see below). Mutual information was
323 estimated using a box kernel-estimator (Kantz and Schreiber, 2003) with a kernel width of 0.5 standard
324 deviations of the data.

325 Here we assume that the neural system is at least capable of exploiting the statistics arising from the
326 stimulation given throughout the experiment and thus construct PDFs from all data (time points and pixels)
327 for a given condition. Therefore, we pool data over the full time course from -1 to 1 second of the
328 experiment. Thus, each image of the VSD data had a spatial configuration of 67x137 spatial data pixels
329 after removal of the 2 rows/columns on each side of an image because of the median filter that was applied.
330 Each trial (of a total of 8 trials per condition) resulted in 288 LAIS values, based on an original data length
331 of 298 samples and a history length (state dimension) of 10 pixels. The product of final image size and
332 LAIS samples resulted in $2.64 \cdot 10^6$ data points per trial for the estimation of the PDF for each of the 8
333 motion direction conditions. Due to computational limitations, LAIS estimates were performed on two
334 blocks of four trials separately, resulting in $1.06 \cdot 10^7$ data points entering the estimation in JIDT.

2.5 CORRELATION ANALYSIS OF LAIS AND VSD DATA

335 For each of the 7 analyzed motion direction conditions, VSD data and LAIS were initially organized
336 separately per condition into 5 dimensional data structures, with dimensions: blocks (1,2), trials (1-
337 4), time (-1 to 1 s), and pixel row (67) and columns (137). For correlation analysis, these arrays
338 were linearized and entered into a Spearman rank correlation analysis to obtain correlation coefficients
339 $\rho(\text{VSD,LAIS})$ and significance values.

Table 1. Correlation of LAIS and local VSD activity (*= $p < 0.05/7$)

Motion direction	Corr. coeff full epoch	Corr. coeff. -1s to 0	Correlation coefficient 0.04 to 0.14 s	0.2 to 1 s
0°	0.05*	-0.33*	-0.09*	0.45*
4 °	0.09*	-0.50*	-0.20*	0.65*
90°	0.12*	-0.30*	-0.13*	0.48*
180°	0.07*	-0.27*	-0.22*	0.44*
225°	0.07*	-0.58*	-0.22*	0.71*
270°	0.17*	-0.39*	-0.33*	0.68*
315°	0.03*	-0.37*	-0.17*	0.40*

Correlation coefficients are Spearman rank correlations.

3 RESULTS

340 LAIS values exhibited a clear spatial and temporal pattern. The temporal pattern exhibited higher LAIS
 341 values during stimulation with a moving random dot pattern than under baseline stimulation with an
 342 isoluminant grey screen, with effects being largest in spatially clearly segregated regions (Figure 1, 2,
 343 3). The spatial pattern of LAIS under stimulation was dependent on the motion direction of the drifting
 344 random dots in the stimulus (Figure 2).

345 In contrast to this spatially highly selective elevation of LAIS values under stimulation, there was a sharp
 346 drop in LAIS values at approximately 40 ms after stimulus onset, with negative LAIS values measured at
 347 many pixels (Figure 1, 40 ms window; Figure 2, middle column; Figure 3, lower row). This indicates that
 348 the baseline activity was misinformative about the following stimulus related activity (since an observer
 349 would expect the baseline activity to continue). This transient, stimulus induced drop in LAIS was more
 350 evenly distributed throughout the imaging window than the elevated LAIS in the later stimulus period
 351 post 200 ms (Figure 2, middle column). The transient drop in LAIS had a recovery time of approximately
 352 34 ms, also giving an estimate of the dominant intrinsic storage duration of the neural processes.

353 In all conditions we observed a positive, but weak correlation between the local VSD activity values and
 354 LAIS values over time and space (Table 1). Looking at individual time intervals, we found stronger, and
 355 negative, correlation coefficients both, for the baseline interval (-1 to 0 s), and for the initial interval after
 356 the onset of the moving dot stimulus (0.04 to 0.14 s). In contrast, we observed a strong positive correlation
 357 at the late stimulus interval (0.2 to 1 s). This means that the increased dynamic range observed in the VSD
 358 signals during stimulation with the moving stimuli led to an increased amount of predictable information,
 359 rather than to a decrease. This correlation also means that storage was generally higher in neurons that
 360 were preferentially activated by the respective moving stimulus (also compare left and right columns in
 361 Figure 2 for each motion direction).

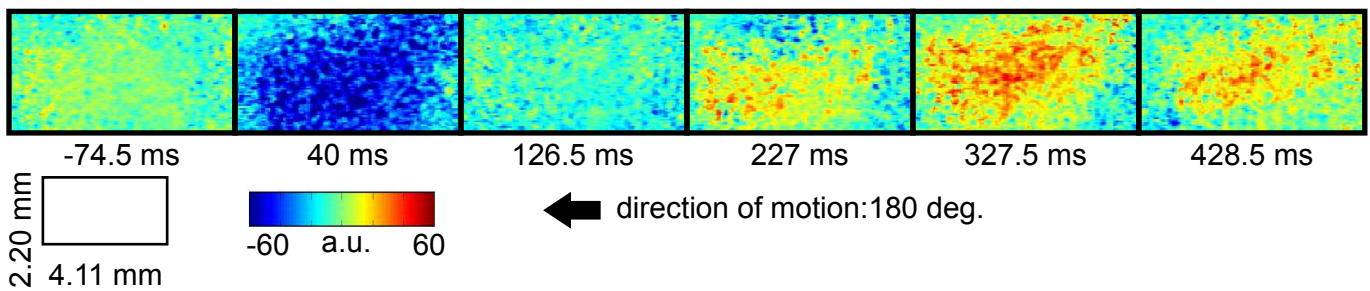


Figure 1. Local active information storage (LAIS) allows to trace neural information processing in space and time. Spatio-temporal structure of LAIS in cat area 18 – seven frames from the spatio-temporal LAIS data, taken at the times indicated below each frame. Stimulation onset was at time 0. Baseline activity (-74.5 ms) is around zero and mostly uniform. At 40 ms after stimulus onset, LAIS is negative in a region that correlates to the region that later exhibits high LAIS. Around 227 ms increased LAIS sets in and lasts until the end of the data epoch, albeit with slow fluctuations (up to 1 s, see Figure 3). Also see the post-stimulus time-average in Figure 2.

4 DISCUSSION

362 Our results demonstrate increased local active information storage in the primary visual cortex of the cat
 363 under sustained stimulation, compared to baseline. The spatial pattern of the LAIS increase was clustered
 364 spatially and stimulus-specific (Figure 2). The temporal pattern of LAIS consisted of a first sharp drop in
 365 LAIS from 0.04 to 0.14 s after onset of the moving stimulus and a sustained rise in LAIS up to the end of
 366 the stimulation epoch ((Figure 3). The sharp drop at stimulus onset for many pixels is important because it
 367 indicates the past activity of the pixels was surprising or misinformative about the next outcomes near that
 368 onset. This has the potential to be used in detecting changes of processing regimes directly from neural
 369 activity.

370 The subsequent sustained rise in LAIS is particularly notable because of the *random spatial* structure of
 371 each stimulus on a local scale; this random spatial structure translates into a random temporal stimulation
 372 sequence in the receptive field of each neuron because of the stimulus motion. The increased LAIS despite
 373 random stimulation of the neurons suggests that our observation is not due to input-driven storage, i.e.
 374 memory or storage contained already in the spatio-temporal stimulus features that drive the observed LAIS
 375 (as discussed in Section 2.2.3 and by **Obst et al.** (2013)). Nevertheless, as revealed by correlation analysis,
 376 storage was highest in regions preferentially activated by the stimulus, suggesting a representational nature
 377 of LAIS in these data with respect to the motion features of the stimulus. In sum, the changes of LAIS with
 378 stimulation onset, stimulation duration, and stimulus type clearly demonstrate that LAIS reflects neural
 379 processing, rather than mere physiological or instrumentation-dependent noise regularities. This leads us
 380 to believe that LAIS is a promising tool for the analysis of neural data in general, and of VSD data in
 381 particular.

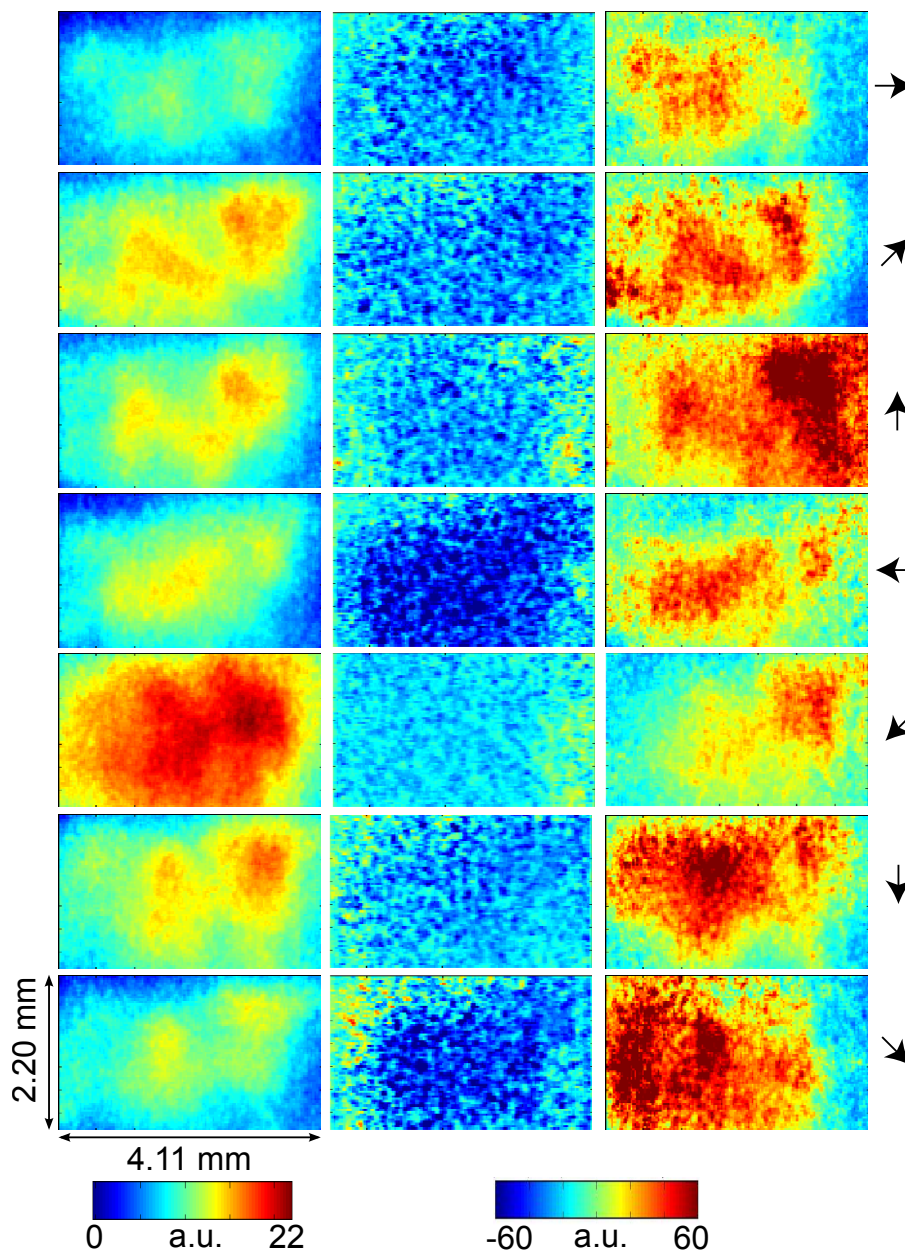


Figure 2. VSD-activity and local active information storage (LAIS) maps. VSD activity averaged over stimulation epochs and time after stimulus onset after the initial transient (0.2-1s) (left column). LAIS map immediately after stimulus onset – negative values (blue) indicate surprise of the system (middle column). Time-average LAIS maps from the stimulus period after the initial transient (0.2-1s) (right column). Rows 1-7 present different stimulus motion directions: 0, 45, 90, 180, 225, 270, 315 (in degrees, indicated by arrows on the right, arrow colors match time-trace colors in Figure 3). 67x137 data pixel per image, pixel dimension $30 \times 32 \mu\text{m}^2$. Left-right image direction is anterior-posterior direction.

4.1 LOCAL ACTIVE INFORMATION STORAGE AND NEURAL ACTIVITY LEVELS

382 Any increase in LAIS may in principle arise from two sources: First, a richer dynamics with a larger
 383 amplitude range – increasing overall information content, while maintaining the predictability of the time

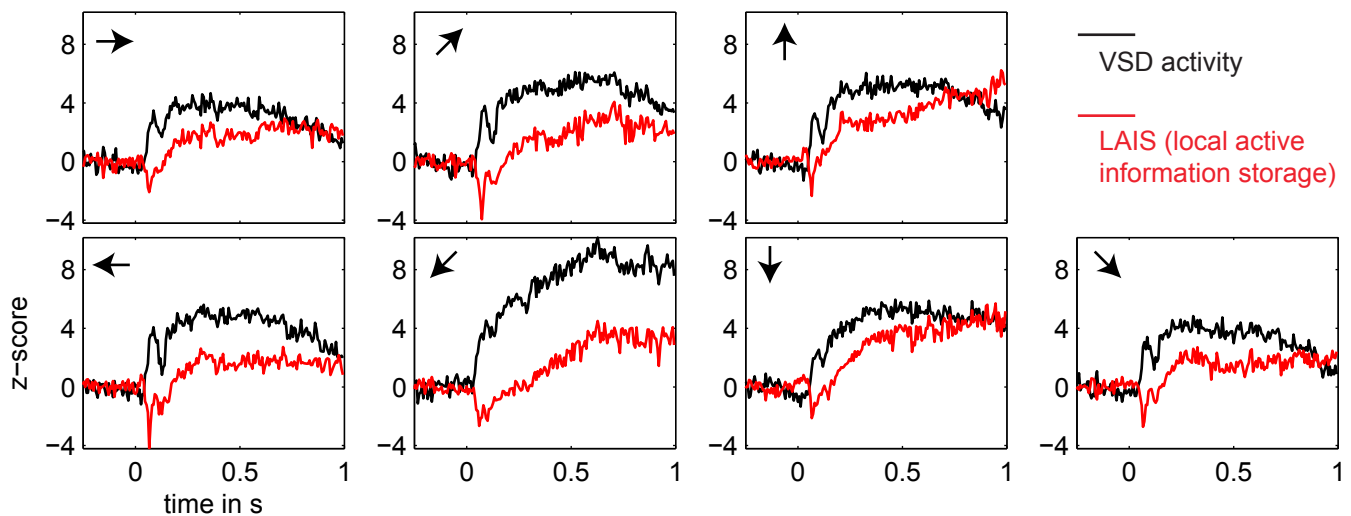


Figure 3. Temporal evolution of VSD activity and local active information storage. Spatial averages over the 67x137 data pixels for VSD activity (black traces), and the LAIS (red traces) versus time. Motion directions are indicated by arrows for each panel. Note that LAIS for the vertical, the right, and the downward-right motion directions continues to rise towards the end of the stimulus interval, despite declining activity levels. Also note that the unexpected onset response at approximately 40 ms leads to negative active information storage. For an explanation see the Methods section.

384 series (e.g. quantified as the inverse of the signal prediction error, or the entropy-normalized LAIS), may
 385 increase LAIS. Alternatively, increased LAIS may be based on increased predictability under essentially
 386 unchanged dynamics. The significant positive correlation between LAIS and VSD activity after stimulus
 387 onset suggests that a richer, but still predictable, dynamics of VSD activity is at the core of the stimulus-
 388 dependent effects observed here. As a caveat we have to note that the use of a kernel estimator for LAIS
 389 measurement, coupled with pooling of observations over the whole ensemble of pixels and time points
 390 may also have introduced a slight bias in favor of a positive correlation between high VSD activity and
 391 LAIS, as it allows storage to be more easily measured in pixels with larger amplitude here. The negative
 392 correlation observed in the baseline interval, however, demonstrates that this bias is not a dominant effect
 393 in our data. This is because a dominant effect of the kernel-based bias would also assign higher storage
 394 values to high amplitude data in the baseline interval, and thereby result in a positive correlation in the
 395 baseline. This was not the case. The relatively low correlation coefficients across the complete time-
 396 interval, which are between 0.02 and 0.13, further suggest that LAIS increases due not follow higher
 397 VSD tightly. Therefore, LAIS extracts additional useful information about neural processing. This point
 398 is further supported by the stimulus-dependent changes that seem more pronounced in LAIS maps than in
 399 the VSD activity maps (compare left and right columns in Figure 2).

400 For future studies the amplitude-bias problem introduced by the fixed-width kernel estimator should
 401 easily be overcome using a Kraskov-type variable width kernel estimator – see the original work of

402 **Kraskov et al.** (2004), and (**Vicente et al.**, 2011; **Lindner et al.**, 2011; **Wibral et al.**, 2011, 2013; **Lizier**,
403 2012) for implementation details of Kraskov-type estimators. Another possibility would be to condition
404 the analysis on the activity level, as for example done for the transfer entropy measure by **Stetter et al.**
405 (2012).

4.2 TIMESCALES OF LAIS

406 The recovery time of the stimulus-induced, transient drop in LAIS was 34 ms. A drop of this kind means
407 that the activity before the drop (baseline activity) was not useful to predict the activity during the drop
408 (the onset response). This is expected as the stimulus is presented in an unpredictable way to the neural
409 system. However, the recovery time of this drop of approximately 34 ms yields an insight into the intrinsic
410 storage time scales of the neural processes. We note that the observed time-scale corresponds to the high
411 beta frequency band around 29 Hz (1/34 ms). In how far this is an incidental finding or bears significance
412 must be clarified in future studies.

4.3 ON THE INTERPRETATION OF LOCAL ACTIVE INFORMATION STORAGE MEASURES IN NEUROSCIENCE

413 When working with measures from information theory, it is important to keep in mind that the basic
414 definition of information as given by Shannon revolves around the probabilities of events and the
415 possibility to encode something using these events. To separate Shannon information content from
416 information about something (new) in a more colloquial sense, one often also speaks about *potential*
417 or *syntactic* information, when referring to Shannon information content, of *semantic* information when
418 referring to human interpretable information, and last of pragmatic information for our everyday notion
419 of information as in 'news' (for details see for example the treatment of **Deacon** (2010) on this topic). In
420 the same way, LAIS does not directly describe information that the neural system stores about things in
421 the outside world – rather, it quantifies how much of the future (Shannon) information in the activity can
422 be predicted from its past.

423 In fact, information in the neural system *about* something in the outside world would have to be
424 quantified by some kind of mutual information between aspects of the outside world and neural activity,
425 while information in the classic sense of semantic information represented symbolically (e.g. in books,
426 and other media) would be even more complicated: theoretically it should be quantified as a mutual
427 information between the medium containing the symbols and activity in the neural system, while
428 additionally satisfying the constraint that this mutual information should vanish when conditioning on
429 the states of the world variables represented by the symbols.

430 While this lack of a more semantic interpretation of LAIS may seem disappointing at first, the
431 quantification of the predictable amount of information makes this measure highly useful in understanding
432 information processing at a more abstract level. This is important wherever we have not yet gained
433 insights into what (if anything) may be explicitly represented by a neural system. Moreover, the focus
434 on predictability provides a non-trivial link between LAIS and current theories of brain function as
435 pointed out below. Nevertheless, a use of the concept in neuroscience may have to take the properties
436 of the receiving neuron or brain area into account to consider how much of the mathematical storage in a
437 signal is accessible to neural information processing. To address this concern, we used a pooling over all
438 available data in space and time here as it seems to represent a way by which a receiving brain area could
439 construct its (implicit) guesses of the underlying probability densities. However, also other strategies are
440 possible and need to be explored in the future. As one example for another strategy of probability-density
441 estimation, we have investigated a construction of probability densities via pooling over all data pixels
442 but separately for each point in time. This approach avoids any potential issues with nonstationarities, but
443 obscures the view of the 'typical transitions' in the system over time to a point that no interpretable results
444 were obtained (data not shown).

4.4 LOCAL ACTIVE INFORMATION STORAGE AND PREDICTIVE CODING THEORIES

445 Information storage in neural activity means that information from the past of a neural process will predict
446 some non-zero fraction of information in the future of this process. It is via this predictability improvement
447 that information storage is also tightly connected with predictive coding, an important family of theories
448 of cortical function. Predictive coding theories propose that a neural system is constantly generating
449 predictions about the incoming sensory input (**Rao and Ballard, 1999; Bastos et al., 2012; Friston,**
450 **2005; Knill and Pouget, 2004**) to adapt internal behavior and processing accordingly. These predictions
451 of incoming information must be implemented in neural activity, and they typically need to be maintained
452 for a certain duration – as it will typically be unknown to the system when the predictive information will
453 be needed. Hence, the neural activity subserving prediction must itself have a predictable character, i.e.
454 non-zero information storage *in activity*. Analysis of active information storage may thereby enable us to
455 test central assumptions of predictive coding theories rather directly. This is important because tests of
456 predictive coding theories so far mostly relied on the predictions being explicitly known and then violated
457 – a condition not given for most brain areas beyond early sensory cortices, and for most situations beyond
458 simple experimental designs. Here, the quantification of the predictability of brain signals themselves
459 via LAIS may open a second approach to testing these important theories. To this end we may scan
460 brain signals for negative LAIS, as negative LAIS values indicate the past states of the neural signals in
461 question were not informative about the future, i.e. negative LAIS signals a breakdown of predictions. In
462 our example dataset this was brought about by the sudden, unexpected onset of the stimulus. However, the

463 same analyses may be applied in situations that are not a under external control – for example to analyze
464 internally driven changes in information processing regimes.

465 In relation to predictive coding theories it is also encouraging that the predictive information was found
466 on timescales related to the beta band. This is because this frequency band has been implied in the intra-
467 cortical transfer of predictions (**Bastos et al.**, 2012).

4.5 SUB-SAMPLING AND COARSE GRAINING, AND NON-LOCALITY OF PDF ESTIMATION

468 When interpreting LAIS values it should be kept in mind that in neural recordings we typically do not
469 observe the system fully or at the relevant scales – in contrast to artificial systems, such as cellular
470 automata and robots, where the full system is accessible. More precisely, in neural data one of two
471 types of sub-sampling is typically present – either coarse graining with local averaging of activity indices
472 (as in VSD) or sub-sampling proper, where neural activity is recorded faithfully (e.g. via intracellular
473 recordings) but with incomplete coverage of the full system. This sub-sampling may have non-trivial
474 effects on the probability distributions of neural events (see for example (**Priesemann et al.**, 2009, 2013)).
475 Hence, LAIS values obtained under sub-sampling should be interpreted as *relative* rather than absolute
476 measures and should only be compared to other experiments, or experimental conditions, when obtained
477 under identical sampling conditions.

478 In addition there is necessarily temporal subsampling in the form of finite data; we therefore note again
479 the potential for bias in the actual MI values returned via the use of kernel estimation here, particularly
480 for large embedding dimensions and small kernel widths. Alternatives to kernelestimators are known
481 to be more effective in bias compensation (e.g. Kraskov-Grassberger-Stögbauer estimation (**Kraskov
482 et al.**, 2004)); or use of use kernel estimation is solely motivated by practical computational reasons.
483 Effects of temporal subsampling also mandates to focus on relative rather than absolute values within this
484 experiment.

485 Even within the experiment though, the bias may not be evenly distributed amongst the local MI values,
486 which tend to exhibit larger bias for low frequency events. With that said, our experiment did use a large
487 amount of data (by pooling observations over pixels and time), which counteracts such concerns to a
488 large degree, and many of the key results (e.g. Figure 3) involve averaging or correlating over many
489 local values, which further ameliorates this. There are techniques suggested to alleviate bias in local or
490 pointwise MI, e.g. (**Turney and Pantel**, 2010), and while none were applied here, we do not believe this
491 alters the general conclusions of our experiment for the aforementioned reasons. As a particular example,
492 the surprise caused by the onset of stimulus is still clearly visible as negative LAIS, despite any propensity
493 for such low frequency events to have been biased strongly towards positive values.

4.6 ON THE LOCALITY OF INFORMATION VALUES

494 As a concluding remark, we would like to point out again that various 'levels of locality' have to be
 495 carefully chosen in the analysis of neural data. One important level is the spatial extent (ensemble of
 496 agents) and the time span over which data are pooled to obtain the PDF. However, even pooling over a
 497 large spatial extent, i.e. many agents and a long time span, may still allow to interpret the information value
 498 of the data agent-by-agent and time step-by-time step, if agents i are *identical* and samples at subsequent
 499 time points t come from a *stationary* random process (see the book of **Lizier** (2013) for several examples).
 500 This is because one may pool data to estimate a PDF as long as these data can be considered 'replications',
 501 i.e. as coming from the same random variable. Pooling data under these conditions will obviously not bias
 502 the PDF estimate away from the ground truth for any agent or time step. Irrespective of how many data
 503 points are pooled this way, it is then still possible to interpret each data point $(x_{i,t}, \mathbf{x}_{i,t-1}^{k-})$ individually in
 504 terms of its LAIS, $a(x_t, \mathbf{x}_{t-1}^{k-})$. This locality of information values is identical to the local interpretation
 505 of the (Shannon) information terms $h(x_i) = -\log(p(x_i))$ that together, as a weighted average over all
 506 possible outcomes x_i , yield the (Shannon) entropy $H(X) = \sum_i p(x_i)h(x_i)$ of a random variable X . As
 507 explained for example by **MacKay** (chapter 4, 2003), each and every outcome x_i of a random variable X
 508 has its own meaningful Shannon information value $h(x_i)$, that may be very different from that of another
 509 outcome x_j , although repeated draws from this random variable can be considered stationary. It is this
 510 sense of 'local' that gives *local* active information storage its name. In contrast, how locally in space and
 511 time we obtain the PDF is more important for the precision of the LAIS estimates.

512 In the analysis of LAIS from neural data three issues will necessarily blur locality, and impair the
 513 precision of the LAIS estimate to some extent:

- 514 1. If a pool of identical agents i , all running identical stationary random processes X_i , is available, the
 515 only blurring of locality arises due to the intrinsic temporal extent of the state variables. However, the
 516 while the stored information may be encoded in a temporally non-local state \mathbf{x}_{t-1}^{k-} , this information
 517 is used to predict the next value of the process x_t at a *single* point in time.
- 518 2. If agents are non-identical, but their data are pooled nonetheless, then the overall empirical PDF
 519 obtained across these agents is no longer fully representative of each single agent and the local
 520 information storage values per agent are biased due to the use of this non-optimal PDF. This effect
 521 may be present to some extent in our analysis, as we cannot guarantee that all parts of area 18 behave
 522 strictly identical.
- 523 3. If the random process in question is not stationary, then a PDF obtained via pooling samples across
 524 time is also not representative of what happens at single points in time, and again a bias in the LAIS
 525 values for each agent and time step arises. This bias is potentially more severe. Nevertheless, we

526 pooled data across all available time samples here, as this seems to be closer to the strategy available
527 to a neuron in a downstream brain area (also see section 2.2.5), when trying to estimate, or adapt
528 to, its input distribution. This is because a neuron may more easily estimate approximate PDFs of
529 its inputs across time than across all possible neurons in an upstream brain area, to most of which it
530 simply doesn't interface.

4.7 CONCLUSION

531 Distributed information processing in neural systems can be decomposed into component processes of
532 information transfer, storage and modification. Information storage can be quantified locally in space
533 and time using an information theoretic measure termed local active information storage (LAIS). Here
534 we present for the first time the application of this measure to neural data. We show that storage reflects
535 neural properties such as stimulus preferences and surprise, and reflects the abstract concept of an ongoing
536 stimulus despite the locally random nature of this stimulus. We suggest that LAIS will be a useful quantity
537 to test theories of cortical function, such as predictive coding.

DISCLOSURE/CONFLICT-OF-INTEREST STATEMENT

538 The authors declare that the research was conducted in the absence of any commercial or financial
539 relationships that could be construed as a potential conflict of interest.

ACKNOWLEDGEMENT

540 The authors thank Matthias Kaschube from the Frankfurt Institute for Advanced Studies (FIAS) for
541 fruitful discussions on active information storage.

542 *Funding:* MW, VP were supported by LOEWE Grant “Neuronale Koordination Forschungsschwerpunkt
543 Frankfurt (NeFF)”. MW thanks the Commonwealth Scientific and Industrial Research Organisation
544 (CSIRO) for supporting a visit in Sydney which contributed to this work. SV was supported by the
545 Bernstein Focus: Neurotechnology (BFNT) Frankfurt/M.

REFERENCES

- 546 Ay, N. and Polani, D. (2008), Information flows in causal networks, *Adv. Complex Syst.*, 11, 17
547 Bastos, A. M., Usrey, W. M., Adams, R. A., Mangun, G. R., Fries, P., and Friston, K. J. (2012), Canonical
548 microcircuits for predictive coding, *Neuron*, 76, 4, 695–711

- 549 Butts, D. A. (2003), How much information is associated with a particular stimulus?, *Network*, 14, 2,
550 177–187
- 551 Butts, D. A. and Goldman, M. S. (2006), Tuning curves, neuronal variability, and sensory coding., *PLoS*
552 *Biol*, 4, 4, e92, doi:10.1371/journal.pbio.0040092
- 553 Cover, T. M. and Thomas, J. A. (1991), Elements of information theory (Wiley-Interscience, New York,
554 NY, USA)
- 555 Crutchfield, J. P. and Feldman, D. P. (2003), Regularities unseen, randomness observed: Levels of entropy
556 convergence, *Chaos*, 13, 1, 25–54, doi:10.1063/1.1530990
- 557 Dasgupta, S., Wörgötter, F., and Manoonpong, P. (2013), Information dynamics based self-adaptive
558 reservoir for delay temporal memory tasks, *Evolving Systems*, 1–15
- 559 Deacon, T. W. (2010), Information and the Nature of Reality (Cambridge University Press), chapter 8
560 What is missing from theories of information?, 146
- 561 DeWeese, M. R. and Meister, M. (1999), How to measure the information gained from one symbol.,
562 *Network*, 10, 4, 325–340
- 563 Faes, L., Nollo, G., and Porta, A. (2012), Non-uniform multivariate embedding to assess the information
564 transfer in cardiovascular and cardiorespiratory variability series., *Comput Biol Med*, 42, 3, 290–297,
565 doi:10.1016/j.compbimed.2011.02.007
- 566 Faes, L., Porta, A., Rossato, G., Adami, A., Tonon, D., Corica, A., et al. (2013), Investigating
567 the mechanisms of cardiovascular and cerebrovascular regulation in orthostatic syncope through an
568 information decomposition strategy, *Autonomic Neuroscience*
- 569 Fano, R. (1961), Transmission of information
- 570 Friston, K. (2005), A theory of cortical responses., *Philos Trans R Soc Lond B Biol Sci*, 360, 1456,
571 815–836, doi:10.1098/rstb.2005.1622
- 572 Gómez, C. and Hornero, R. (2010), Entropy and complexity analyses in alzheimers disease: An MEG
573 study, *The open biomedical engineering journal*, 4, 223
- 574 Granger, C. W. J. (1969), Investigating causal relations by econometric models and cross-spectral
575 methods., *Econometrica*, 37, 424–438
- 576 Kantz, H. and Schreiber, T. (2003), Nonlinear Time Series Analysis (Cambridge University Press), 2
577 edition
- 578 Knill, D. C. and Pouget, A. (2004), The bayesian brain: the role of uncertainty in neural coding and
579 computation., *Trends Neurosci*, 27, 12, 712–719, doi:10.1016/j.tins.2004.10.007
- 580 Kraskov, A., Stoegbauer, H., and Grassberger, P. (2004), Estimating mutual information., *Phys Rev E Stat*
581 *Nonlin Soft Matter Phys*, 69, 6 Pt 2, 066138
- 582 Langton, C. G. (1990), Computation at the edge of chaos: Phase transitions and emergent computation,
583 *Physica D: Nonlinear Phenomena*, 42, 1, 12–37

- 584 Lindner, M., Vicente, R., Priesemann, V., and Wibral, M. (2011), Trentool: A Matlab open source toolbox
585 to analyse information flow in time series data with transfer entropy., *BMC Neurosci*, 12(119), 1, 1–22,
586 doi:10.1186/1471-2202-12-119
- 587 Lizier, J. T. (2012), JIDT: An information-theoretic toolkit for studying the dynamics of complex systems,
588 <http://code.google.com/p/information-dynamics-toolkit/>
- 589 Lizier, J. T. (2013), The Local Information Dynamics of Distributed Computation in Complex Systems.,
590 Springer theses (Springer)
- 591 Lizier, J. T., Atay, F. M., and Jost, J. (2012a), Information storage, loop motifs, and clustered structure in
592 complex networks., *Phys Rev E Stat Nonlin Soft Matter Phys*, 86, 2 Pt 2, 026110
- 593 Lizier, J. T., Flecker, B., and Williams, P. L. (2013), Towards a synergy-based approach to measuring
594 information modification, in Proceedings of the 2013 IEEE Symposium on Artificial Life (ALIFE)
595 (IEEE), 43–51, doi:10.1109/alife.2013.6602430
- 596 Lizier, J. T. and Prokopenko, M. (2010), Differentiating information transfer and causal effect, *Eur. Phys.*
597 *J. B*, 73, 605–615
- 598 Lizier, J. T., Prokopenko, M., and Zomaya, A. Y. (2012b), Local measures of information storage in
599 complex distributed computation, *Information Sciences*, 208, 39–54, doi:10.1016/j.ins.2012.04.016
- 600 MacKay, D. J. (2003), Information theory, inference and learning algorithms (Cambridge university press)
- 601 Mitchell, M. (1998), Computation in cellular automata: A selected review, in T. Gramß, S. Bornholdt,
602 M. Groß, M. Mitchell, and T. Pellizzari, eds., Non-Standard Computation (Wiley-VCH Verlag GmbH
603 & Co. KGaA, Weinheim), 95–140, doi:10.1002/3527602968.ch4
- 604 Mitchell, M., Hraber, P., and Crutchfield, J. P. (1993), Revisiting the edge of chaos: Evolving cellular
605 automata to perform computations, *arXiv preprint adap-org/9303003*
- 606 Obst, O., Boedecker, J., Schmidt, B., and Asada, M. (2013), On active information storage in input-driven
607 systems, arXiv:1303.5526
- 608 Pincus, S. M. (1991), Approximate entropy as a measure of system complexity., *Proceedings of the*
609 *National Academy of Sciences*, 88, 6, 2297–2301, doi:10.1073/pnas.88.6.2297
- 610 Porta, A., Baselli, G., Liberati, D., Montano, N., Cogliati, C., Gnecci-Ruscione, T., et al. (1998),
611 Measuring regularity by means of a corrected conditional entropy in sympathetic outflow., *Biological*
612 *Cybernetics*, 78, 1, 71–78
- 613 Porta, A., Guzzetti, S., Montano, N., Pagani, M., Somers, V., Malliani, A., et al. (2000), Information
614 domain analysis of cardiovascular variability signals: evaluation of regularity, synchronisation and co-
615 ordination, *Medical and Biological Engineering and Computing*, 38, 2, 180–188
- 616 Priesemann, V., Munk, M. H. J., and Wibral, M. (2009), Subsampling effects in neuronal avalanche
617 distributions recorded in vivo., *BMC Neurosci*, 10, 40, doi:10.1186/1471-2202-10-40

- 618 Priesemann, V., Valderrama, M., Wibral, M., and Le Van Quyen, M. (2013), Neuronal avalanches differ
619 from wakefulness to deep sleep—evidence from intracranial depth recordings in humans., *PLoS Comput*
620 *Biol*, 9, 3, e1002985, doi:10.1371/journal.pcbi.1002985
- 621 Prokopenko, M., Boschiatti, F., and Ryan, A. J. (2009), An Information-Theoretic primer on complexity,
622 Self-Organization, and emergence, *Complexity*, 15, 1, 11–28
- 623 Prokopenko, M., Gerasimov, V., and Tanev, I. (2006), Evolving spatiotemporal coordination in a modular
624 robotic system, in S. Nolfi, G. Baldassarre, R. Calabretta, J. C. T. Hallam, D. Marocco, J.-A. Meyer,
625 O. Miglino, and D. Parisi, eds., From Animals to Animats 9: Proceedings of the Ninth International
626 Conference on the Simulation of Adaptive Behavior (SAB'06), volume 4095 of *Lecture Notes in*
627 *Computer Science* (Springer, Berlin Heidelberg), 558–569, doi:10.1007/11840541_46
- 628 Ragwitz, M. and Kantz, H. (2002), Markov models from data by simple nonlinear time series predictors
629 in delay embedding spaces., *Phys Rev E Stat Nonlin Soft Matter Phys*, 65, 5 Pt 2, 056201
- 630 Rao, R. P. and Ballard, D. H. (1999), Predictive coding in the visual cortex: a functional interpretation of
631 some extra-classical receptive-field effects., *Nat Neurosci*, 2, 1, 79–87, doi:10.1038/4580
- 632 Richman, J. S. and Moorman, J. R. (2000), Physiological time-series analysis using approximate entropy
633 and sample entropy, *American Journal of Physiology - Heart and Circulatory Physiology*, 278, 6,
634 H2039–H2049
- 635 Schreiber (2000), Measuring information transfer, *Phys Rev Lett*, 85, 2, 461–464
- 636 Stetter, O., Battaglia, D., Soriano, J., and Geisel, T. (2012), Model-free reconstruction of excitatory
637 neuronal connectivity from calcium imaging signals., *PLoS Comput Biol*, 8, 8, e1002653, doi:10.1371/
638 journal.pcbi.1002653
- 639 Takens, F. (1981), Detecting strange attractors in turbulence, in D. Rand and L.-S. Young, eds., Dynamical
640 Systems and Turbulence, Warwick 1980, volume 898 of *Lecture Notes in Mathematics* (Springer, Berlin
641 / Heidelberg), chapter 21, 366–381
- 642 Turing, A. M. (1936), On computable numbers, with an application to the Entscheidungsproblem,
643 *Proceedings of the London mathematical society*, 42, 2, 230–265
- 644 Turney, P. D. and Pantel, P. (2010), From frequency to meaning: Vector space models of semantics,
645 *Journal of Artificial Intelligence Research*, 37, 141–188+, doi:10.1613/jair.2934
- 646 Vakorin, V. A., Mii, B., Krakovska, O., and McIntosh, A. R. (2011), Empirical and theoretical aspects of
647 generation and transfer of information in a neuromagnetic source network., *Front Syst Neurosci*, 5, 96,
648 doi:10.3389/fnsys.2011.00096
- 649 Vicente, R., Wibral, M., Lindner, M., and Pipa, G. (2011), Transfer entropy – a model-free measure of
650 effective connectivity for the neurosciences., *J Comput Neurosci*, 30, 1, 45–67
- 651 Wang, X. R., Miller, J. M., Lizier, J. T., Prokopenko, M., and Rossi, L. F. (2012), Quantifying and tracing
652 information cascades in swarms., *PLoS One*, 7, 7, e40084, doi:10.1371/journal.pone.0040084

-
- 653 Wibral, M., Pampu, N., Priesemann, V., Siebenhner, F., Seiwert, H., Lindner, M., et al. (2013),
654 Measuring information-transfer delays., *PLoS One*, 8, 2, e55809, doi:10.1371/journal.pone.0055809
- 655 Wibral, M., Rahm, B., Rieder, M., Lindner, M., Vicente, R., and Kaiser, J. (2011), Transfer entropy
656 in magnetoencephalographic data: Quantifying information flow in cortical and cerebellar networks.,
657 *Prog Biophys Mol Biol*, 105, 1-2, 80–97
- 658 Wiener, N. (1956), The theory of prediction., in E. F. Beckmann, ed., In *Modern Mathematics for the*
659 *Engineer* (McGraw-Hill, New York)
- 660 Zipser, D., Kehoe, B., Littlewort, G., and Fuster, J. (1993), A spiking network model of short-term active
661 memory, *The Journal of Neuroscience*, 13, 8, 3406–3420